Paper ID APEN-MIT-2022_8513
Applied Energy Symposium: MIT A+B
July 5-8, 2022 • Cambridge, USA

Effect of spray nozzle parameters on surface wettability and performance improvement of indirect evaporative cooler

Xiaochen Ma*
Department of Building Environment and Energy Engineering
The Hong Kong Polytechnic University
Hong Kong, China
xiaochencc.ma@connect.polyu.hk

Wenchao Shi
Department of Building Environment and Energy Engineering
The Hong Kong Polytechnic University
Hong Kong, China
wenchao511.shi@connect.polyu.hk

Hongxing Yang*
Department of Building Environment and Energy Engineering
The Hong Kong Polytechnic University
Hong Kong, China
hong-xing.yang@polyu.edu.hk

Abstract— Indirect evaporative cooling (IEC) is a well-known sustainable cooling technology that can potentially replace mechanical cooling equipment and operate as an efficient energy recovery unit or standalone cooling system. However, the technology relies heavily on water evaporation in the wet channels to cool the fresh air in the adjacent channel. Although many moisture-absorbing materials have been proposed for IEC to improve the surface wettability, the uneven water membrane coverage caused by inappropriate nozzle parameters is still a great problem that degrades the evaporation. Therefore, it is critical to optimize the nozzle parameters in water spray systems and arrange the nozzles reasonably above the IEC for more efficient evaporation performance. In this research, a novel 3D simulation model describing the vapor and liquid phase distribution from the spray system was developed to allow a comprehensive parametric study based on Computational Fluid Dynamics (CFD). A test rig of an open-circuit wind tunnel was built to measure the actual wetted areas on the surface of a single channel pair for model validation. The results based on the verified simulation model showed that the water membrane coverage ratio could achieve the optimal value of 0.21 as the droplet diameter was 0.05 mm. Furthermore, the wet-bulb efficiency of the IEC with a size of $260 \times 400 \times 400$ mm^3 could reach a maximum value of 52%, supported by two spray nozzles 160 mm apart with a droplet size of 0.05 mm.

Keywords—indirect evaporative cooler, CFD model, water membrane, nozzle parameters, optimization

I. INTRODUCTION

Currently, the building sector has already surpassed commercial and public services as the major energy consumers, accounting for 26.9% of worldwide energy consumption [1]. In Hong Kong, 50% of building energy consumption comes from indoor air conditioning and cooling, which emerged as one of the largest drivers of electricity consumption rise [2]. Meanwhile, the growing worries of the public about indoor air quality as well as thermal comfort have increased energy consumption for cooling and dehumidifying outdoor air in buildings [3]. Therefore, it is critical to promote sustainable cooling technology vigorously to reduce electricity demand. By utilizing the latent heat of water evaporation, IEC systems consume less energy and emit less greenhouse gas., attracting the attention of a large number of related researchers [4].

The most essential thermodynamic process for IEC is the evaporation process occurred in wet channels, which cools the plate surface and drives a significant amount of heat to be transferred from the dry to the wet side [5]. Generally, the greater cooling efficiency of the cooler will be achieved by higher water evaporation rate [6]. To enhance the evaporation process occurred in wet channels, a lot of research has been conducted on the material and structure of the channel plate. Antonellis et al. [7] indicated that a reticular plate protrusion guaranteed a higher heat transfer rate than the flat plates and formed a more uniform water layer than the complex plates. Guilizzoni et al. [8] applied a novel material with hydrophilic characteristics on the surface of the plate, which could promote the wet-bulb effectiveness by up to 10%. However, almost all of these solutions have the drawback of high workload and relatively high cost.

The arrangement parameter of spray nozzles is another hot issue that has attracted a lot of attention. Sun et al. [9] proved that cooling efficiency only increased with the spraying water flow rate in a certain range through experiments. Antonellis et al. [10] have also investigated five alternative water nozzle arrangements on an IEC to determine which had the maximum wet-bulb efficiency while consuming the least amount of water. It is found that a better spray arrangement can produce larger contact areas and less heat transfer resistance between the two airflows. Ma et al. [11] tested the performance of optimized nozzle arrangement on IEC based on the proposed numerical model, which proved that a reasonable arrangement scheme could improve wet-bulb efficiency to 16%.

However, some issues persist in the actual operation of a popular IEC product, causing major water evaporation concerns, such as: 1) the sprayed water droplets in unfavorable sizes can cause the drift, in which the liquid particles are carried out by the leaving air stream without evaporation; 2) the water membrane on the plate surface will not be ideal because of the water surface tension and different nozzle working conditions; 3) large unwetted dry regions on the plates cut down the effective heat transfer areas for water evaporation.

Due to the complexity of the spraying droplet movement in the narrow channels and evaporated by the air stream, the numerical study of the water distribution system of IEC can be a challenge. Montazeri et al. [12] conducted Computational Fluid Dynamics (CFD) simulations on an evaporative cooling system, in which the Lagrangian-Eulerian principle was used to assess the two-phase flow in a spray system. However, this simulation study is based on direct evaporative cooling without considering the effects of the heat exchanger and the droplets impingement on the wet channel surfaces. For the IEC, there is still a lack in the persuasive simulation models of water spraying systems that consider both the atomized droplets and the film formed on the channel surfaces. In order to fill this gap, this paper developed a 3D CFD simulation model for the description of water spraying distribution and the formation of water membrane. The model will be verified and then applied to evaluate the effect of different nozzle parameters on IEC performance. Finally, the optimal design for nozzle parameters and the optimized IEC efficiency improvement will be provided. A flow chart is displayed in Fig. 1 to help comprehend the current investigation.

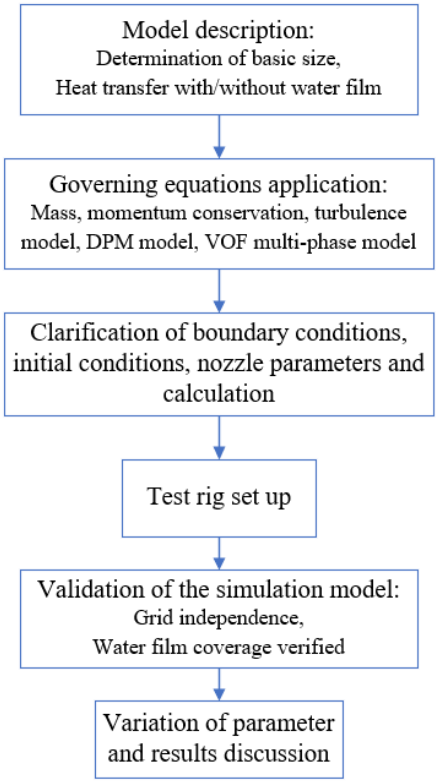

Fig. 1 Flow chart of this research

II. MODEL DESCRIPTION

The CFD model was created in the commercial software Space claim in the ANSYS, and the details of the simulation model will be described below.

A. *Model geometry and computational grid*

There are many wet channels for water evaporation in an IEC heat exchanger. To save computer space, it was assumed that the identical circumstance occurred in each wet channel, hence just one typical channel was examined. The IEC was reduced to a single wet channel of 4 × 400 mm, as illustrated in Fig. 2. A solid cone nozzle was set 150 mm above the plate, and counter current flow configuration between water and gas was arranged in the channel. A continuous stream of droplets sprayed by the nozzle falls into the wet channel one after another, and some of them come into contact with the plate to form a water membrane and then flow down the flat surface. Meanwhile, secondary air flowed up the wet channel from the bottom to the top, making contact with the liquid film going downward.

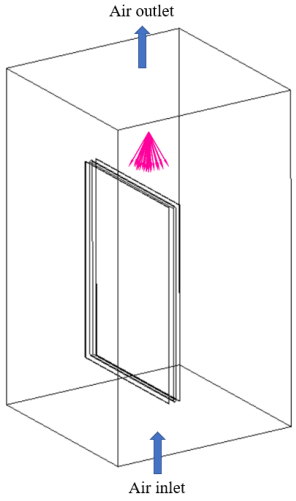

Fig. 2 A typical channel in the IEC

According to the previous research carried out by Yang et al. [13], the physical model showed a different heat and mass transfer between wet and dry areas as depicted in Fig .3.

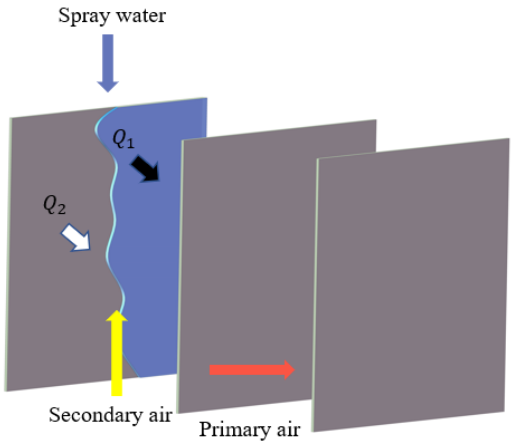

Fig. 3 Physical model of plate type cross-flow IEC

In a real situation, the spray water can not completely wet the plate surface of the wet channels ideally because of the high surface tension of the water. Thus, a coverage factor should be utilized to quantify the impact of the partial wetting area, which is named as a ratio of the wet area allocated on the whole plate, shown in Eq. (1) [13].

$$\varphi = \frac{A_w}{A_{pl}} \tag{1}$$

where φ is the coverage ratio of the wet channels; A_w is wet area for membrane evaporation; A_{pl} is the whole plate area.

B. *Model equations*

The distribution of the vapor and liquid phases of the spray system within the IEC is governed by the conservation principles. The following are the detailed formulations for these conservation principles:

(1) Conservation of mass

$$\frac{\partial}{\partial t}(\rho) + \nabla \cdot (\rho u) = 0 \quad (2)$$

where ρ represents density ($\mathrm{kg} \cdot m^{-3}$), and u represents velocity ($m \cdot s^{-1}$).

(2) Conservation of momentum

$$\frac{\partial}{\partial t}(\rho E) + \nabla \cdot (\rho u^2) = -\nabla P + \nabla \cdot \left(\mu(\nabla u + \nabla u^T)\right) + \rho g + F \quad (3)$$

where P represents pressure (Pa), μ represents dynamic viscosity ($\mathrm{kg} \cdot m^{-1} \cdot \mathrm{s}^{-1}$), F is the source objective of the momentum equation ($N \cdot m^{-3}$).

(3) Mass transfer

$$h_{ms}\left(\omega_{t_w} - \omega_s\right)\sigma \cdot dxdy = \dot{m}_s \frac{\partial \omega_s}{\partial y} \cdot dy \quad (4)$$

$$\frac{\partial \omega_e}{\partial y} = \dot{m}_s \frac{\partial \omega_s}{\partial y} \quad (5)$$

(4) VOF multi-phase model

Equations (6) and (7) explain the density and viscosity of each numerical grid in the VOF model.

$$\rho = \alpha_1 \rho_1 + \alpha_g + \rho_g \quad (6)$$

$$\mu = \alpha_1 \mu_1 + \alpha_g + \mu_g \quad (7)$$

$$\frac{\partial \alpha_{1/g}}{\partial t} + \vec{u} \cdot \nabla \alpha_{1/g} = 0 \quad (8)$$

(5) Discrete phase (spray droplets) model

The nozzle spray situation above the heat exchanger was achieved by DPM model in this research, and the stochastic collision, coalescence as well as breakup elements were considered.

As a result, inertia, gas phase aerodynamic drag force, combined with gravity will affect discrete phase droplets. The following force balance equation can be used to calculate the trajectory of droplets using a combined Euler-Lagrangian approach.

$$\frac{d\left(\overrightarrow{X_g}\right)}{dt} = \overrightarrow{V_g} \quad (9)$$

where $\vec{V}_d$ represents the velocity of droplet (m/s); and $\vec{X}_d$ represents the position of droplet (m).

The velocity of an evaporating circular water particle travelling in a continuous airflow was predicted according to Newton's second equation of motion. The heat and mass exchange with air is aided by the two-way coupling of air and droplets. The movement equation for a single droplet is defined as:

$$\frac{d\left(m_d \overrightarrow{F_d}\right)}{dt} = \overrightarrow{F_D} + \overrightarrow{F_g} \quad (10)$$

The drag force applies in the opposite direction of the relative velocity of the droplet to the wind. The resistance to drag is determined by the shape and size of the spray droplet, its relative velocity in relation to the air, and the density of the air [14]. The drag coefficient takes into consideration all of these impacting elements. The drag force for a spherical drop is

$$\vec{F}_d = -\frac{\pi}{8} C_D \rho_a D_d^2 \vec{V}_r \left|\vec{V}_r\right| \quad (11)$$

where C_D represents the drag coefficient and $\vec{V}_r$ is the droplet relative velocity ($m \cdot s^{-1}$).

(6) Turbulence model

The following equation described the calculation method of the Reynolds number.

$$Re_s = 4\bar{\omega}\delta/v \quad (12)$$

where Re_s represents the flow Reynolds number, dimensionless, $\bar{\omega}$ is the longitudinal velocity, $m \cdot s^{-1}$, and δ is the film thickness, m.

In this research, the $k - \varepsilon$ turbulence model was used because of the characteristics of low-Reynolds-number flow.

C. Boundary conditions and simulation settings

In this research, the commercial CFD software Fluent was applied to simulate the continuous formation of water membrane during the spray period. Fig. 4 illustrated the meshing sketch applied in this model. The boundary conditions for each objective in the simulation model are indicated as follows. All of the sides surrounding were set as the adiabatic wall. The three middle plates were regarded as the absorbed wall, with the trap of DPM and boundary conditions of Eulerian wall film model (EWF). The top side was set as an air inlet, and correspondingly the bottom was the air outlet.

Considering the actual state of droplets sliding down the plate surface after forming a film on the plate surface, the model calculation here needs to consider the influence factors of gravity force, surface shear force and surface tension. Besides, The SIMPLE and the highly recommended PRESTO! pressure interpolation systems were utilized to decouple the pressure and velocity equations.

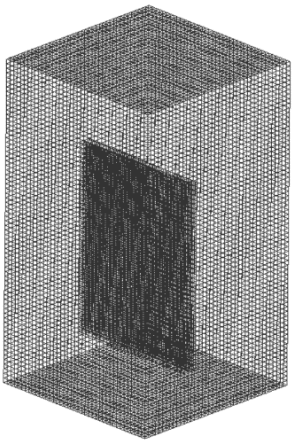

Fig. 4 Sketch of meshing in the model

III. EXPERIMENT AND VERIFICATION

A. Introduction of experimental system

To verify the proposed 3D simulation model, a test rig was arranged and set up as shown in Fig. 5. Three main elements

were included in this whole system, namely heat exchanger, water supply unit and air supply unit. The heat exchanger, which is a critical component of IEC, is made up of alternate dry and wet channels. The plates of the IEC are separated by neatly spaced inward and outward microscopic projections, providing a 4 mm channel gap for the airflows, with a dimension of 0.26 m × 0.4 m × 0.4 m. As the spray water was supported by the above nozzle, the cool and dry secondary airflow is reversed from bottom to top with the spray droplets. At this time, the spray droplets will make contact with the plate surface of heat exchanger, and the droplets that meet the conditions will accumulate to form a water film. A transparent plate covers the outer secondary air channel in the heat exchanger, allowing visualization of the water membrane distribution on the heat exchanger plate. Sliding nozzles were mounted on top of the heat exchanger to simulate the effect of spray on the water membrane distribution on the surface of heat exchanger plate at different distances.

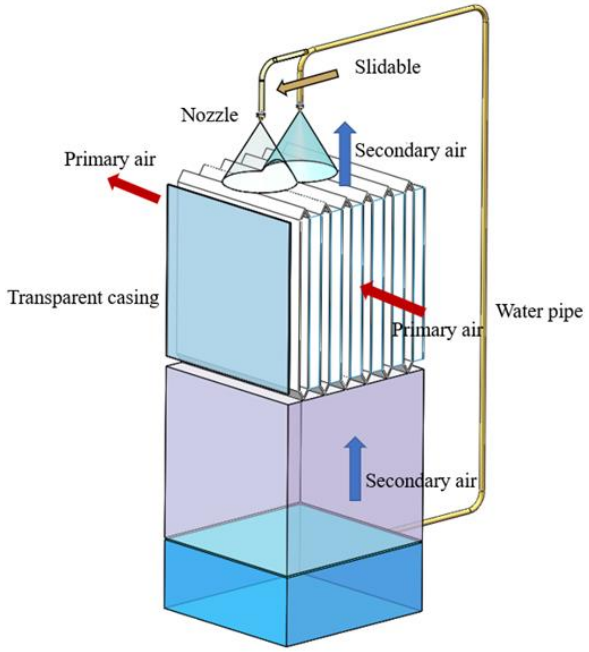

Fig. 5 Test rig

B. *Model Validation*

1) *Grid independence*

The ICEM software in ANSYS was applied to the mesh computational model. During the simulation period, the water membrane covered the plate of the heat exchanger with such thin film thickness. For the region near the wall, the finite grid with a size less than 0.1 mm was used to catch the flow properties of the thin membrane. In general, as mesh quality improves, the computational accuracy improves. However, the time consumption also increases due to a large amount of mesh grid. Thus, there is a compromise between accuracy and cost of calculation progress, and a reasonable number of meshes is chosen to ensure that the computational accuracy is ideal in the context of the computation.

The coverage ratio under different grid separately were shown in Fig. 6. It is evident that as mesh quality improved, the coverage ratio of the water membrane grew first, and then levelled off at grid number of 113200, which could be decided as the simulation number for further research.

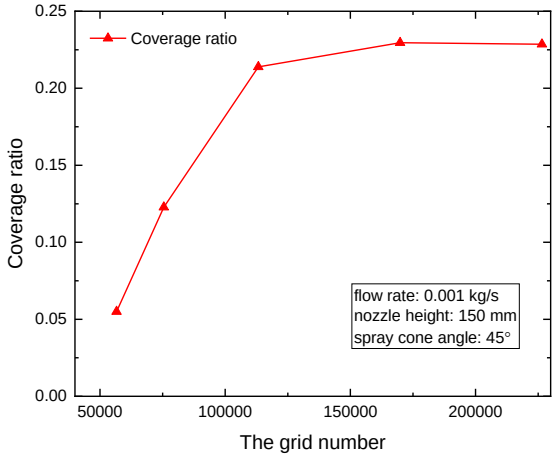

Fig. 6 Coverage ratio at different numbers of grid

2) *Validation*

The proposed water membrane distribution model based on CFD principle was verified in terms of water membrane coverage area. To clarify the water membrane coverage situation on the plate surface, the divided grid will be supplied. The actual division example of the real experimental and simulation results could be seen in Fig. 7 (a) and (b) separately.

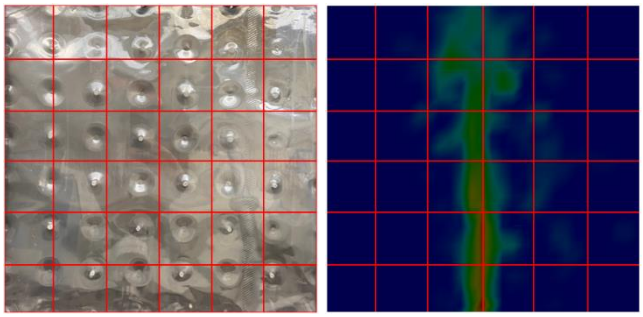

(a) Experiment scenario (b) Simulation scenario

Fig. 7 Illustration of the division example

The numerical model used identical initial parameters to the experimental model. The tests were carried out under the given circumstances: Q = 0.001 kg/s, spray cone angle α = 45°, and nozzle height H = 150 mm. The simulation results of the coverage ratio were compared to the experimental results. As shown in Fig. 8, these points were located within ± 20%, and the maximum discrepancy was observed as 7.1%, which was acceptable for the further analysis.

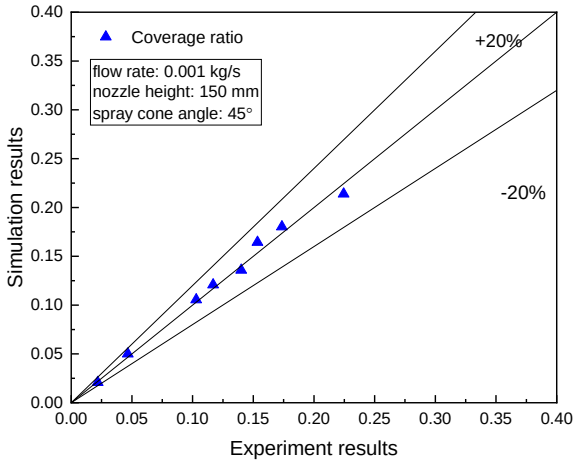

Fig. 8 Comparison between the measured and simulated data

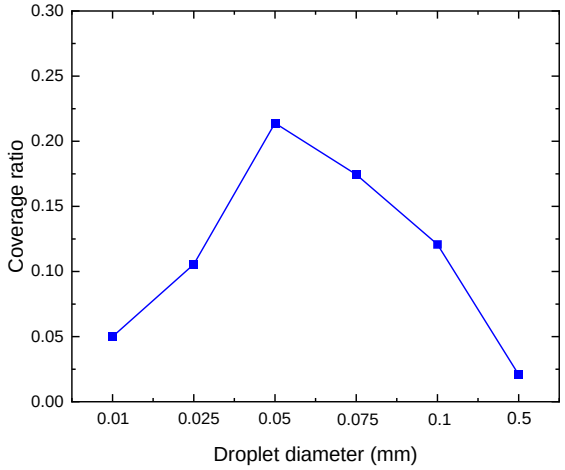

Fig. 9 Influence of droplet diameter on the coverage ratio

IV. RESULTS AND DISCUSSIONS

The verified model was applied to carry out the parametric study to identify the influence of nozzle variations on water membrane distributed on the wet channel plate surface.

A. Influence for single nozzle

The droplet diameter of a nozzle was selected as the first investigated factor, and other influencing factors were set to fixed values as shown in Table I.

TABLE I. OTHER INFLUENCE FACTORS

Parameter	***Nozzle cone angle***	***Flow rate***	***Nozzle height***
Value	45°	0.001 kg/s	150 mm

As can be seen from Fig. 9, the total water membrane coverage area on the plate surface expands sharply with the increase of spray droplet diameter at the beginning of the period and achieves a maximum value of 0.22 at a diameter of 0.05 mm. Subsequently, the area covered by the water membrane gradually decreases with increasing droplet diameter, and there is no further increasing trend.

When the flow rate and height of the spray nozzle are fixed, droplets ejected by the nozzle are too small to be carried by the bottom-up airflow provided in the secondary air channel, resulting in the droplets to be blown away before they come into contact with the plate surface. Conversely, when the droplet diameter is too large, the weight factor could cause it to slide out of the wet channel before making contact with the plate surface. Therefore, an unsuitable droplet size for the same water rate supply will deteriorate the water membrane distribution, while an optimal size value can expand the water film coverage by even 77%.

B. Influence of multi-nozzles

To investigate the effect of the multi-nozzle arrangement scheme on IEC efficiency when optimal injection parameters are adopted at the top of a real-size IEC ($260 \times 400 \times 400$ mm^3), 0.05 mm will be used as the fixed droplet injection particle size.

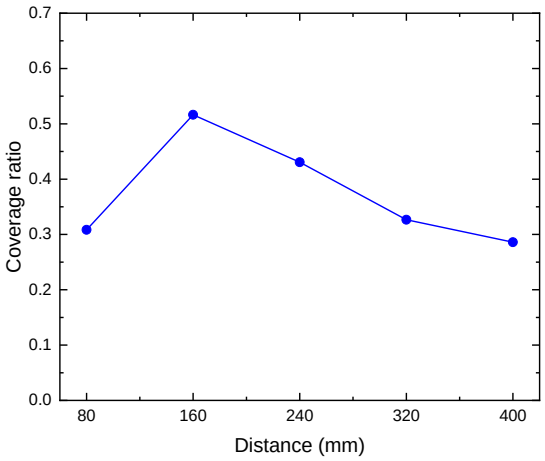

Fig. 10 Influence of nozzle distance on coverage ratio

As depicted in Fig. 10, when the distance between the two nozzles was increased from 80 mm to 160 mm, the water film coverage on the plate surface was expanded from 0.31 to 0.52. However, as the nozzle spacing is greater than 160 mm, the coverage area of the water film decreases in an almost linear trend. This phenomenon is explained by the fact that spray of nozzles are too far apart causing some droplets to escape from the boundary, while being too close caused a large number of spray droplets to collide and splash against each other, making it difficult to touch the plate to form a film.

C. Influence on IEC performance

To assess the influence of the nozzle parameters on the IEC performance, the numerical model developed by Yang et al. [13] was applied here. Fig. 11 shows the wet-bulb effectiveness changed by the droplet diameter produced by the two same nozzles. The highest wet-bulb efficiency value

can be achieved at a spray droplet size of 0.05 mm and a distance of 160 mm, when the wet-bulb efficiency is 52%. This demonstrates that only changing one parameter, the spray droplet size, can achieve an increase in wet bulb efficiency from 34% to 51% by affecting the coverage of the water membrane on the plate surface under the same operating conditions.

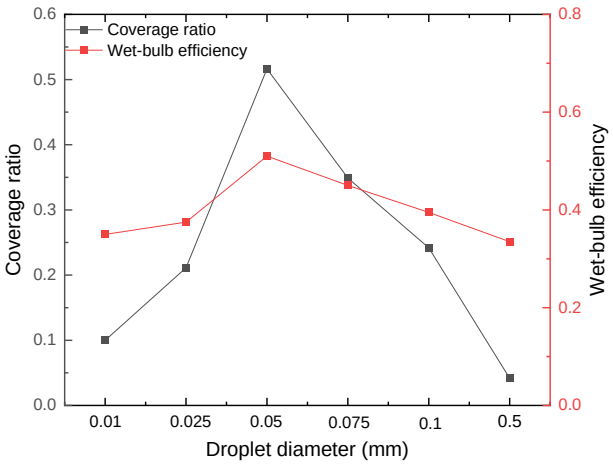

Fig. 11 Influence of droplet diameter on wet-bulb efficiency

V. CONCLUSIONS

In this paper, a 3D CFD model of the water membrane formation influenced by nozzle parameters on a wet channels plate was proposed. The reliability of the model was verified by experimental data. Based on the validated model, the effect of spray droplet diameter on water membrane coverage area and the IEC performance promotion were analysed. The following are the major findings of this research:

1) The water membrane coverage ratio has the highest value when the spray droplet diameter is 0.05 mm, and the value of coverage ratio is 0.22.

2) When the fixed distance between two nozzles are 160 mm, the coverage ratio of the water membrane on the plate surface is optimal, which is up to 0.52.

3) For the IEC with 400 mm length and 260 mm width, two nozzles set 160 mm apart in the nozzle particle size of 0.05 mm can achieve the maximum wet-bulb efficiency of 51%.

4) By appropriately setting the spray droplet parameters to influence the coverage area of the water membrane on the plate surface, the wet-bulb efficiency of IEC can be increased by 17% under the same conditions.

ACKNOWLEDGEMENT

The authors wish to acknowledge the financial support provided by the General Research Fund projects of the Hong Kong Research Grant Council (Ref. No.: 15213219 and 15200420).

REFERENCE

[1] IEA, World electricity final consumption by sector, 2018, IEA, Paris https://www.iea.org/data-and-statistics/charts/world-electricity-final-consumption-by-sector-2018

[2] Pérez-Lombard L, Ortiz J, Pout C. A review on buildings energy consumption information. Energy Build 2008;40:394–8. https://doi.org/10.1016/j.enbuild.2007.03.007.

[3] Sá JP, Alvim-Ferraz MCM, Martins FG, Sousa SIV. Application of the low-cost sensing technology for indoor air quality monitoring: A review. Environ Technol Innov 2022;28:102551. https://doi.org/10.1016/j.eti.2022.102551.

[4] Shi W, Min Y, Ma X, Chen Y, Yang H. Dynamic performance evaluation of porous indirect evaporative cooling system with intermittent spraying strategies. Appl Energy 2022;311:118598. https://doi.org/10.1016/j.apenergy.2022.118598.

[5] Shi W, Min Y, Ma X, Chen Y, Yang H. Performance evaluation of a novel plate-type porous indirect evaporative cooling system: An experimental study. J Build Eng 2021;48:103898. https://doi.org/10.1016/j.jobe.2021.103898.

[6] Yang H, Shi W, Chen Y, Min Y. Research development of indirect evaporative cooling technology: An updated review. Renew Sustain Energy Rev 2021;145:111082. https://doi.org/10.1016/j.rser.2021.111082.

[7] De Antonellis S, Cignatta L, Facchini C, Liberati P. Effect of heat exchanger plates geometry on performance of an indirect evaporative cooling system. Appl Therm Eng 2020;173:115200. https://doi.org/10.1016/j.applthermaleng.2020.115200.

[8] Guilizzoni M, Milani S, Liberati P, De Antonellis S. Effect of plates coating on performance of an indirect evaporative cooling system. Int J Refrig 2019;104:367–75. https://doi.org/10.1016/j.ijrefrig.2019.05.029.

[9] Sun T, Huang X, Chen Y, Zhang H. Experimental investigation of water spraying in an indirect evaporative cooler from nozzle type and spray strategy perspectives. Energy Build 2020;214:109871. https://doi.org/10.1016/j.enbuild.2020.109871.

[10] S. De Antonellis S, Joppolo CM, Liberati P, Milani S, Romano F. Modeling and experimental study of an indirect evaporative cooler. Energy Build 2017;142:147–57. https://doi.org/10.1016/j.enbuild.2017.02.057.

[11] Ma X, Shi W, Yang H. Study on water spraying distribution to improve the energy recovery performance of indirect evaporative coolers with nozzle arrangement optimization. Appl Energy 2022;318:119212. https://doi.org/10.1016/j.apenergy.2022.119212.

[12] Montazeri H, Blocken B, Hensen JLM. Evaporative cooling by water spray systems: CFD simulation, experimental validation and sensitivity analysis. Build Environ 2015;83:129–41. https://doi.org/10.1016/j.buildenv.2014.03.022.

[13] Yang M, Ma H, Ma S, Nong A, Zhang Y, Ma Y. Effect of surface wettability on air parameters and performance of indirect evaporative cooler in the presence of primary air condensation. J Build Eng 2022;45:103535. https://doi.org/10.1016/j.jobe.2021.103535.

[14] Yu J, Jin S, Xia Y. Experimental and CFD investigation of the counter-flow spray concentration tower in solar energy air evaporating separation saline wastewater treatment system. Int J Heat Mass Transf 2019;144:118621. https://doi.org/10.1016/j.ijheatmasstransfer.2019.118621.